UFSM

CIÊNCIA e NATURA

ISSN 2179-460X
OPEN ACCESS

Ci. e Nat., Santa Maria, v. 46, spe. n. 1, e86861, 2024 • https://doi.org/10.5902/2179460X86861
Submitted: 27/02/2024 • Approved: 25/06/2024 • Published: 04/11/2024

Special edition ERMAC e ENMC

Dynamics of lithium ions on a silicene anode grown by vapor deposition using Morse and MEAM potentials

Dinâmica de íons de lítio em um ânodo de siliceno crescido por deposição de vapor usando potenciais de Morse e MEAM

Alexandre Melhorance Barboza[I], Luis César Rodríguez Aliaga[I], Daiara Faria[I], Ivan Napoleão Bastos[I]

[I] Universidade do Estado do Rio de Janeiro, Nova Friburgo, RJ, Brazil

ABSTRACT

Silicene, the silicon analogue of graphene, has been theoretically envisioned as a material with great potential applications, especially as an anode in lithium-ion batteries. However, the understanding of its behavior as an anode remains unclear, as research in this area is still in its preliminary phases. Furthermore, existing studies do not account for defects commonly found in silicene layers, which could potentially alter its behavior as an anode. Therefore, this study investigates the dynamics of Li ions on a defective silicene layer using molecular dynamics simulations and two distinct interatomic potentials: Morse and 2NN-MEAM. The results show that with both potentials, Li ions tend to position themselves in the middle of Si rings with six or more elements without significantly deforming the nearby lattice. However, the 2NN-MEAM potential causes severe deformation during Li diffusion on rings with five or less elements, making it impractical to investigate silicene as anode. In contrast, the Morse potential manages to maintain the silicene's structure. Nevertheless, during the insertion of Li ions into the anode's channel, Si adatoms create barriers to Li diffusion, damaging the silicene structure. These results cast uncertainty upon the feasibility of employing silicene as an anode.

Keywords: Silicene; Lithium-ion battery; Molecular dynamics

RESUMO

Siliceno, o análogo de silício do grafeno, foi teoricamente concebido como um material com grande potencial de aplicações, especialmente como anodo em baterias de íons de lítio. No entanto, a compreensão de seu comportamento como anodo ainda não está clara, uma vez que a pesquisa nessa área ainda está em sua fase preliminar. Além disso, estudos existentes não consideram defeitos comumente encontrados em folhas de siliceno, o que poderia potencialmente alterar seu comportamento como anodo. Nesse contexto, este estudo investiga a dinâmica de íons de Li em monocamada de

siliceno defeituoso usando simulações de dinâmica molecular e dois potenciais interatômicos distintos: Morse e 2NN-MEAM. Os resultados mostram que, com ambos os potenciais, os íons de Li tendem a se posicionar no centro dos anéis de Si com seis ou mais elementos sem deformar significativamente a rede cristalina. No entanto, o potencial 2NN-MEAM causa deformação severa durante a difusão de Li em anéis com menos de cinco elementos, tornando impraticável investigar o siliceno como anodo. Em contraste, o potencial Morse permite manter a estrutura do siliceno. Contudo, durante a inserção de íons de Li no canal do anodo, adátomos de Si criam barreiras à difusão de Li, danificando a estrutura do siliceno. Esses resultados lançam incertezas sobre a viabilidade do uso de siliceno como anodo.

Palavras-chave: Siliceno; Bateria de íon de lítio; Dinâmica molecular

1 INTRODUCTION

In recent decades, the rapid advancement of portable electronics, electric vehicles, and renewable energy systems has triggered an ever-growing demand for high-performance energy storage technologies (Luo et al., 2018). Among the various contenders, lithium-ion batteries (LIBs) have emerged as the preferred choice due to their remarkable energy density, long cycle life, and relatively low environmental impact (Galashev, Ivanichkina et al., 2019). However, modern electric and electronic equipment have already demonstrated that the current anode technology employed in the vast majority of these batteries is no longer sufficient to satisfactorily supply certain applications (Marom et al., 2011).

The majority of LIBs currently utilize graphite-based anodes, known for significantly impeding the energy-storage capacity (Han et al., 2021). To address this limitation, scientists have turned to silicon, renowned for its exceptionally high theoretical energy storage capacity (Galashev & Rakhmanova, 2019). However, despite its remarkable potential, silicon experiences rapid capacity decay due to structural deterioration caused by volumetric fluctuations during Li insertion and extraction (Galashev & Rakhmanova, 2019). To overcome these challenges, the adoption of thin films, particularly silicene, presents a promising solution (Salah et al., 2019; Luo et al., 2018).

Silicene is a two-dimensional (2D) allotrope of silicon and, similarly to graphene, consists of a single layer of silicon atoms arranged in a honeycomb lattice. Due to its

unique properties, silicene has broad application in many fields, such as in biomedical applications, chemical sensors, electronic devices, and energy storage (Feng et al., 2014; Liu et al., 2018; You et al., 2021; Barboza et al., 2022). However, despite its excellent theoretical properties, the understanding of physical behavior and synthesis of silicene still remain as challenges to the scientific community (Sassa et al., 2020). Techniques commonly applied to obtain graphene and other 2D materials, such as mechanical exfoliation, cannot be directly applied to silicene, making it necessary to explore new processing routes. To date, the main method for silicene production is the epitaxial growth on metal substrates by the vapor deposition (VD) technique (Zhao et al.,2016). Moreover, only a limited number of substrates allow crystallization of silicene, including Ag, Au, Ir, ZrB_2, ZrC, and MoS_2 (Zhao et al., 2016).

Although some theoretical studies regarding the application of silicene as anode in LIBs exists in the literature (Galashev et al., 2019; Galashev et al. 2020), they do not consider the influence of defects commonly observed in experimental grown of 2D materials, such as grain boundaries (GBs), voids, adatoms and non-six-membered rings. Moreover, the influence of a substrate, necessary for ensuring silicene's mechanical stability, is frequently disregarded.

In this context, this work employs molecular dynamics (MD) simulations to investigate the influence of a silicene with defects, grown by VD technique, on Li ion behavior. Thus, taking into account the defects that are naturally observed in experimental synthesis of 2D materials. Additionally, two distinct interatomic potentials for the Si-Li pairs are employed to eliminate the possibility of an inaccurate description of the system.

2 METHODOLOGY

Molecular dynamics simulations were performed with the LAMMPS code (Thompson et al., 2022), which is a commonly used platform to study solid materials (Andrade, 2020).Due to the absence of a dedicated interatomic potential for the

Au-Si-Li system, a hybrid potential approach was adopted. This encompassed an angular-dependent potential for the Au-Au, Au-Si, and Si-Si pairs (Starikov et al., 2018), a modified embedded atom method (MEAM) for Li-Li pair (Kim et al., 2012), and a Lennard-Jones (LJ) potential for Au-Li pair. The LJ potential was created using the Lorentz-Berthelot mixing rule, with the unary parameter values obtained from the Kim repository (Tadmor et al., 2011). Considering two elements, i and j, their interaction, using the Lorentz-Berthelot rule, can be expressed as (Müser et al., 2022):

$$\sigma_{ij} = \frac{\sigma_i + \sigma_j}{2} \quad (1)$$

$$\varepsilon_{ij} = \sqrt{\varepsilon_i \varepsilon_j} \quad (2)$$

where σ is the distance at which the inter-particle potential is zero, and ε is the depth of the potential well, which is the minimum potential energy when the particles are at an equilibrium distance. The Si-Li pair was described by a second nearest-neighbor modified embedded atom method (2NN-MEAM) (Cui et al., 2012) or Morse potential (Galashev, Katin et al., 2019). The Au substrate was generated with dimensions approximately measuring 230 Å X 230 Å X 12 Å, using the Atomsk software (Hirel, 2015). Spatial configuration and snapshots of the system during simulations were performed with the Ovito Pro (Stukowski, 2010). Periodic boundary conditions were applied to the x– and y–axis, while fixed boundary was established along the z–axis, aligned with the c–direction of silicene. The first two Au atomic layers were maintained fixed in place to avoid sliding, while the rest of the layers were controlled by a Nose-Hoover thermostat. The equations of motion were integrated at intervals of 0.001 ps. Prior to the Si deposition process, an energy minimization step was performed using the conjugate gradient algorithm.

To mimic the growth of silicene with the VP technique, Si atoms were deposited at a constant rate of 1000 atom/ns on the Au substrate maintained at 500 K within a NVT ensemble. A more detailed explanation regarding the growth methodology can

be seen in our previous study (Barboza et al., 2024). After the completion of silicene growth, the temperature was lowered to 300 K to initiate the Li ion insertion. Both Si and Li elements were controlled by a NVE ensemble.

The silicene channel was created by replicating both the substrate and silicene, followed by a 180° rotation. The gap within the channel was established at 7.5 Å, consistent with the parameters utilized in previous research (Galashev et al., 2019).

3 RESULTS

3.1 Silicene sheet geometrical characteristics

The grown silicene layer obtained is presented in Fig. 1. Unlike the pristine structure typically used in MD studies, this sample exhibits multiple defects, some of which are emphasized in the inset of Fig. 1. Additionally, large voids are evidenced after growth, resulting from the non-uniformity grown of islands during the Si deposition process. This type of structure resembles those found in other works using Ir as a substrate (Cherukara et al., 2017). Table 1 presents some characteristics of the silicene sheet.

Figure 1 – Resulting silicene layer after Si deposition onto Au substrate. Blue and yellow spheres represents the Si and Au atoms, respectively. The zoomed area highlights three types of defects, namely adatoms (colored in red), eight-membered rings (colored in green), and seven-membered rings (colored in cyan)

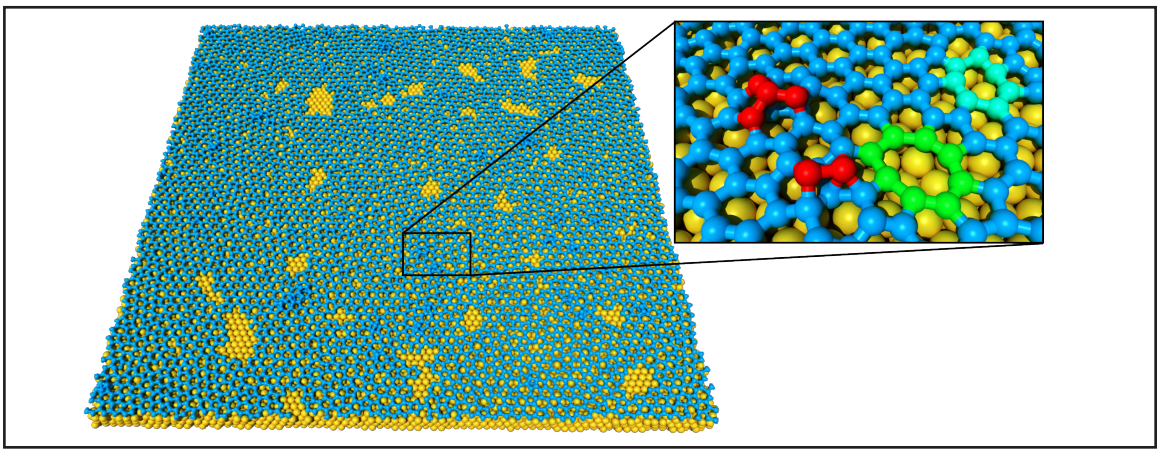

Source: Authors (2023)

Table 1 – Characteristics of the silicene sheet after grown. The bond length and buckling height are presented as average values. The defect value means the absolute count of rings that deviate from the six-membered structure

	Bond length (Å)	Grains	Buckling height (Å)	Six membered rings	Defects
Silicene layer	2.44	10	0.41	3041	309

Source: Athours (2023)

3.2 2NN-MEAM potential

The evolution of Li deposition on the silicene structure using the 2NN-MEAM potential is depicted in the Fig. 2. As can be seen, in the early stages, Fig. 2a-2b, while the density of Li atoms is relatively low (less than 2 %), the integrity of the silicene structure remains intact., i.e., the interaction between the pairs Au-Li and Si-Li is not sufficient to promote bond breakage. During this stage, the Li ions tend to accommodate themselves in the middle of hexagon rings, as depicted in the Fig.3a, without significantly impact the nearby silicene lattice, which is in good concordance with other studies (Zhuang et al., 2017). Given the limited Li density in this stage, these ions can diffuse over the silicene layer in order to find non-defective rings. However, with an increase in Li density, Fig. 2c-2d, maintaining this behavior becomes progressively challenging due to the presence of multiple imperfections within the investigated silicene layer. Eventually, the only viable locations for Li ions to settle into are those containing defects. This fact significantly alters the interaction dynamics among Si-Li pairs, leading to the observation of numerous bond breakages and formations. The resulting structure will be primarily influenced by the specific type of defect present.

In cases where the defects are rings with more than six elements, the Li ions can position themselves within the centers of these rings, similar to their arrangement in non-defective rings, as depicted in Fig. 3b for a seven-membered ring case as example. Conversely, when the defects involve rings with fewer than six members, the Li ions are unable to remain stable atop these rings due to the limited available space,

inducing their diffusion towards the nearest ring with six or more members. However, this displacement is accompanied by a severe distortion in the original five-membered ring, as shown in Fig 3c-3e.

Figure 2 – Evolution of Li ion deposition onto the silicene layer. The Li density, with respect to the Si atoms, is (a) 0.6, (b) 1.2, (c) 4.0, and (d) 7.0 %. The pink spheres represent the Li ions

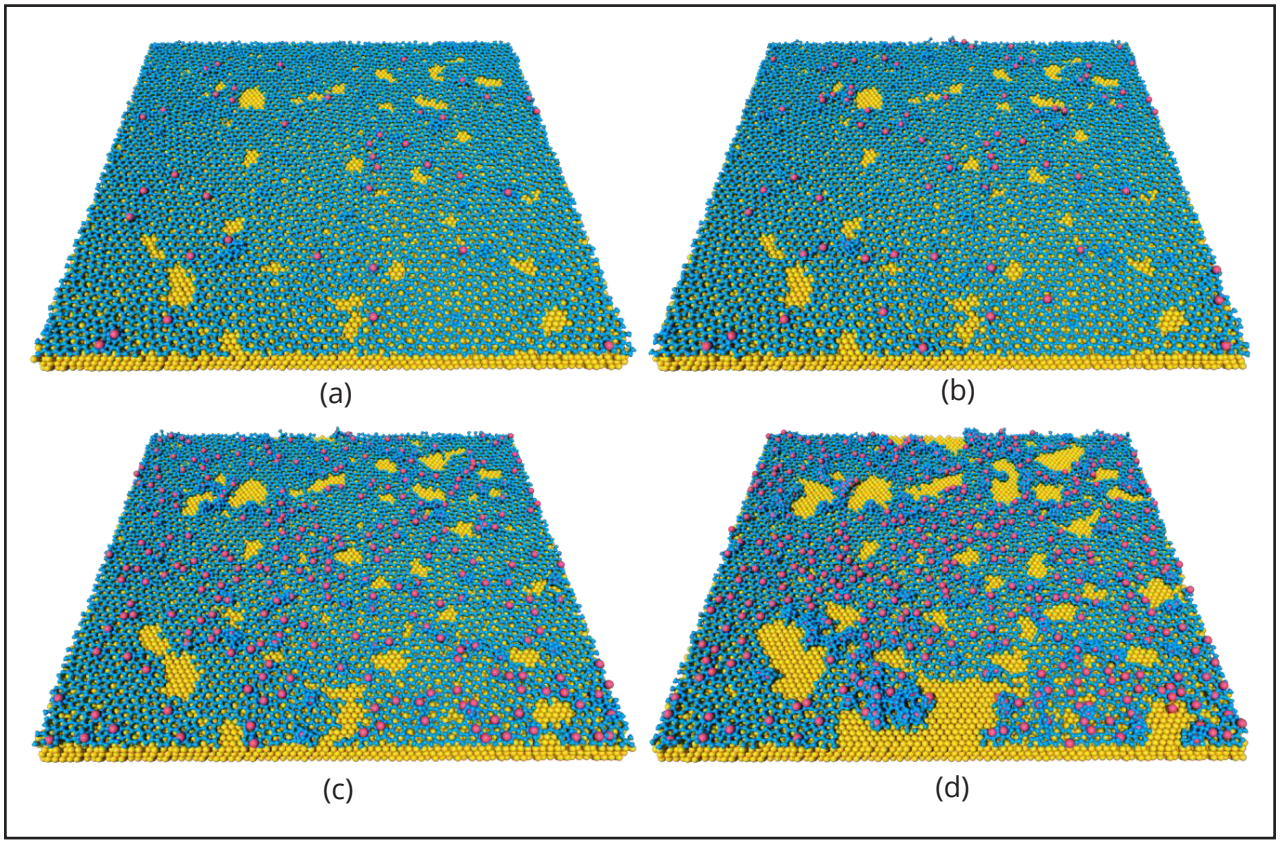

Source: Authors (2023)

As more Li ions are deposited near the already deformed sites, they begin to interact with each other, causing further deformation in the silicene's structure. This pattern is consistently observed when Li ions interact with Si adatom defects. Ultimately, the planar hexagonal configuration of silicene becomes compromised, revealing a collection of Li ions intertwined with Si atoms, as shown in Figure 4.

Figure 3 – Geometrical configuration of a stable Li ion over a (a) six-membered ring and (b) seven-membered ring. Figures (c) - (e) depict the process of lattice deformation induced by a non-stable Li ion over a five-membered ring (colored in orange)

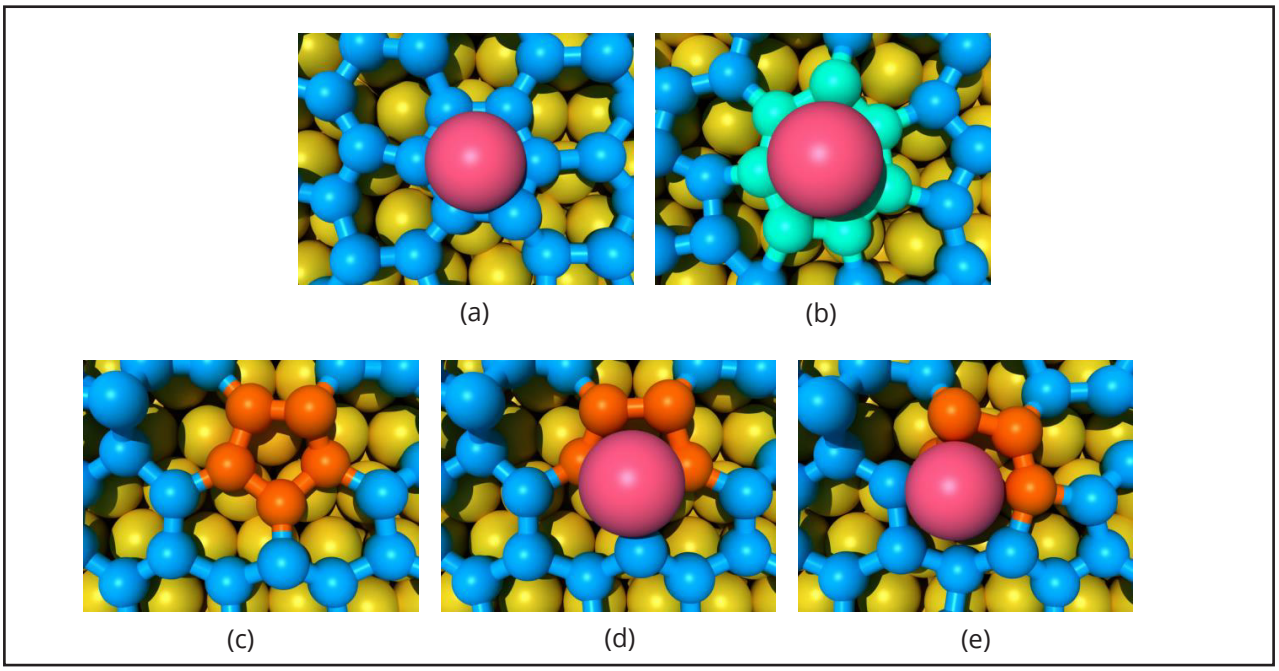

Source: Authors (2023)

Figure 4 – A region of the silicene layer with a Li ion density of 7 % showcasing several Li ions wrapped by Si atoms

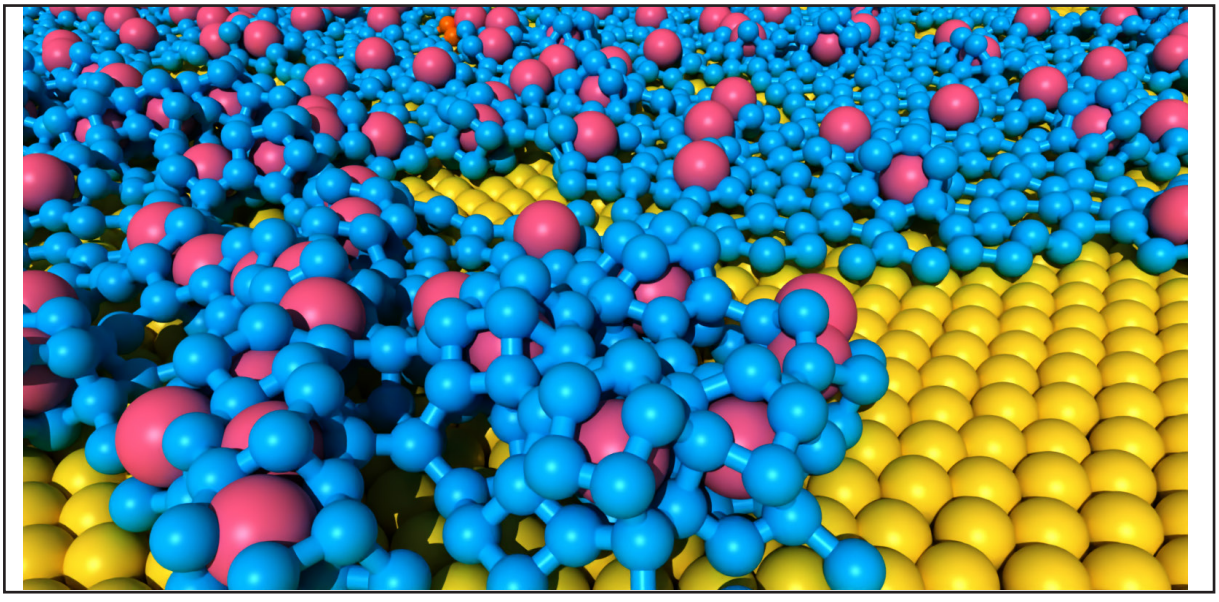

Source: Authors (2023)

It is important to notice that until this point, there is no presence of an electrical field in the system. Not surprisingly, the application of an electric field with the presence of a high density of Li ions causes further deformation in the silicene lattice. This occurs due to the movement of Li ions that are already surrounded by Si atoms, resulting in their interaction with even more Si atoms. This process follows a cascading effect, resembling the way a snowball accumulates as it rolls. In contrast, when examining the scenario with low-density Li ions, the application of an electric field does not induce substantial strain in the silicene layer. This is because the Li ions have not yet become encased by Si atoms.

3.3 Morse potential

The intense lattice strain resulting from Li ion diffusion, as predicted by the 2NN-MEAM potential, seems unlikely to be solely attributed to the interaction between defective rings and Li ions. This is particularly noteworthy given the significantly low diffusion barrier of Li atoms within a thin layer of amorphous silicon (Hüger & Schmidt, 2018). The only plausible explanation for this observation lies in the potential used, which may not accurately capture the interactions within the system. To address this concern, a relatively recently developed Morse potential was employed in lieu of the 2NN-MEAM potential (Galashev, Katin et al., 2019).

Despite its simpler formalism compared to 2NN-MEAM, the Morse potential explicitly provides parameters for a defective silicene, potentially resulting in a more accurate representation of the considered system. Indeed, when conducting the same Si deposition as with the 2NN-MEAM, i.e., with Si ions being deposited at the same place, the final silicene structure remains practically intact even after reaching a density of 7.0% Li ions.

Under the influence of the Morse potential, the behavior of Li ions closely resembles that observed with the 2NN-MEAM potential. They exhibit a tendency to transition from rings composed of five or fewer elements to those with six or more elements. However, this diffusion is not accompanied by deformation of silicene's

lattice, indicating that the attractive force of the Morse potential is less pronounced and more accurate than that of the 2NN-MEAM one. To measure the potential energy during diffusion, Li ions were conveniently positioned on each ring type (ranging from four- to eight-membered rings) and also on the Au substrate, which is accessible within the void regions. These mentioned results are presented in Fig. 5.

Figure 5 – Energy variation of Li ions during diffusion. At the initial time, the Li ions are precisely positioned on the designated ring or substrate

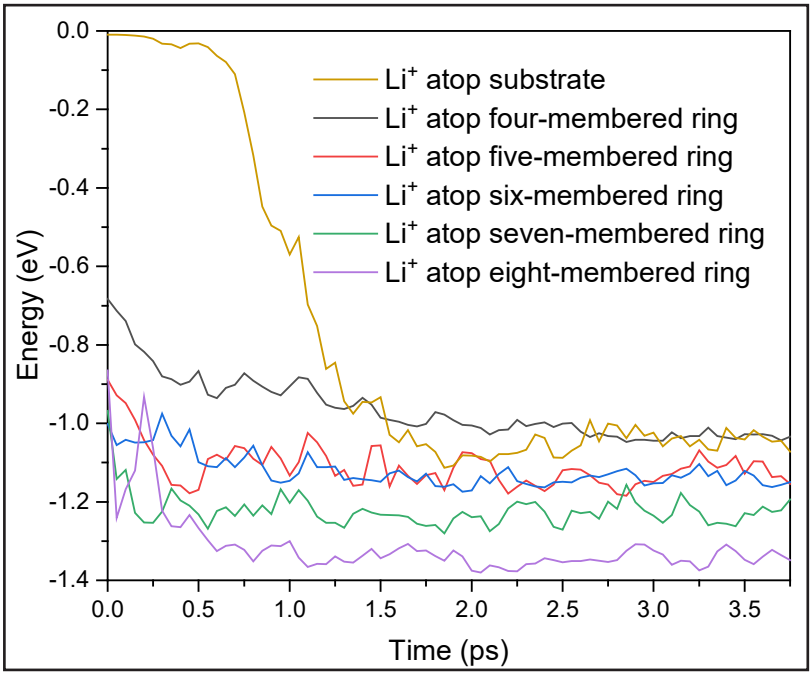

Source: Authors (2023)

As observed in Fig. 5, the energy profiles show the tendency of Li ions to migrate to rings comprising six or more elements. While the Li ions on the substrate migrated to a six-membered ring, this ring is adjacent to a void. Consequently, it possesses higher potential energy when compared to a perfect six-membered ring since it is bonded with other rings where not all Si atoms are connected to three other Si atoms; only two are connected. The eight-membered ring exhibited the lowest energy, followed by the seven, six, and five-membered rings. The adatom on a four-membered ring failed to diffuse to a six or higher-membered ring. This ring is also adjacent to a void, thus displaying higher potential energy, close to the one that originated on the substrate. Despite all Li ions

being placed at the same absolute height, the relative height between Li and Si differs for each one due to non-uniform atomic vibrations and the inherent buckling height of silicene. Therefore, certain outlying energy peaks in the initial stage (time < 0.5 ps) are caused by this fact, as observed at 0.25 ps for the eight-membered ring.

With the Morse potential, it is possible to further explore the interaction of Li ions by considering a silicene anode.

3.4 Silicene anode

The most basic theoretical representation of an anode is a channel consisting of two layers separated by a specific distance. In this case, the distance used is 7.5 Å, as also utilized in other works (Galashev, Ivanichkina et al., 2019). Figure 6(a) presents a channel view normal to the $y-z$ plane, with Li ions introduced at the beginning of the channel along the $x-$axis. In Figure 6(b), two distinct paths, namely, clean and dirty, are shown. It is important to note that the top portion of the anode was removed to ease visualization.

These paths were named based on the quantity of defects along the way. The clean path exhibits few defects, and those that exist do not include adatoms. In contrast, the dirty path has several defects, including clusters of adatoms, as evidenced in the zoomed area in Fig. 6(a). Our interest in these scenarios is to investigate the isolated behavior of Li ions in both paths under the influence of a constant electric field. Specifically, we aim to understand how defects can impact the insertion of Li ions.

In search for the optimal electrical field strength, a single Li ion was introduced into the clean channel of silicene at the mean height between the top and bottom silicene layers. Various electric field strengths, applied solely along the $x-$axis, were utilized, and the corresponding positions and velocities of the Li ion were computed. It is noteworthy that the electric field affected only the Li ions, each possessing an electric charge of $1e$, where e represents the elementary electric charge. The results are presented in Fig. 7.

Figure 6 – Silicene anode with (a) lateral view showcasing the channel gap of 7.5 Å and (b) an isometric view demarcating two Li ions paths, namely dirt and clean. The zoomed area highlights the barrier to Li movement create by adatoms defect

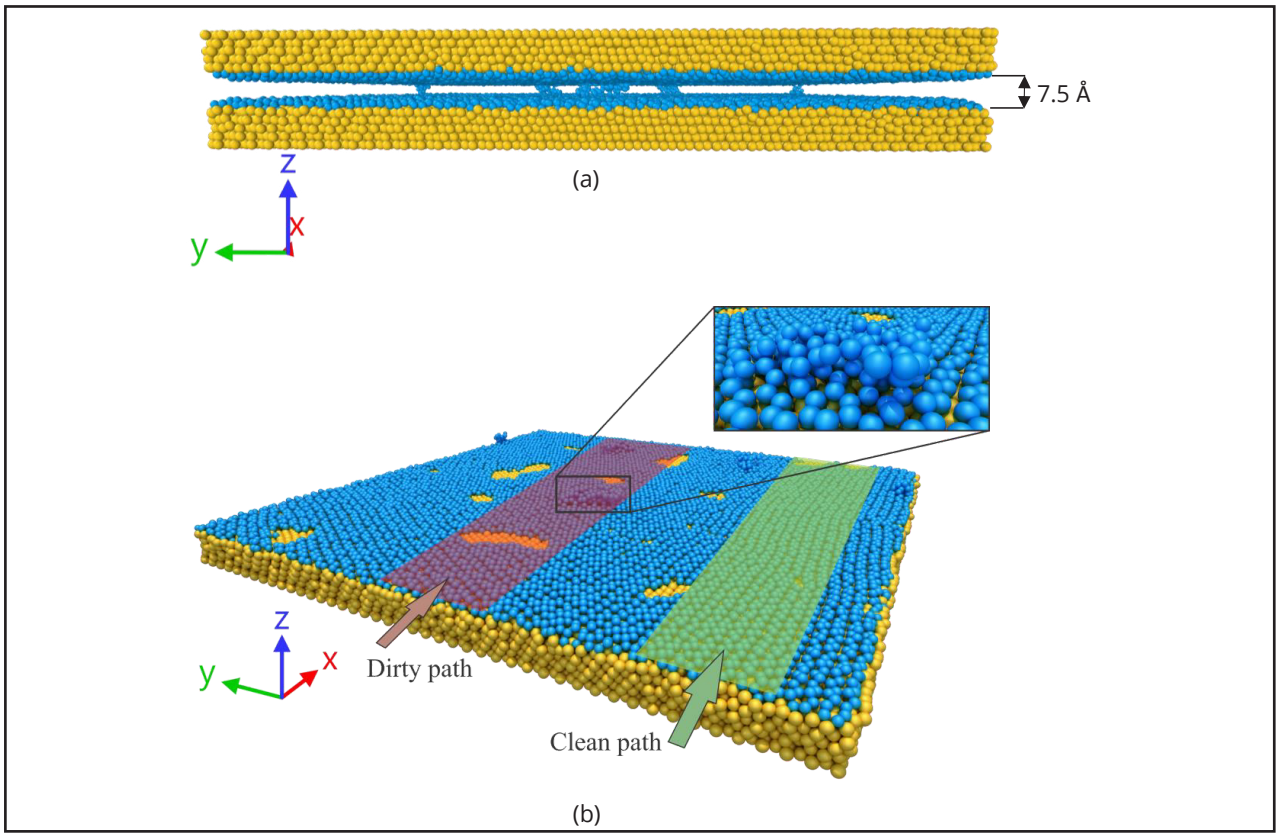

Source: Authors (2023)

Figure 7 – Evolution of Li ion with time under the influence of different electrical fields. The position of Li ion in (a) is relative to the length traversed along the x–axis, and (b) shows the correspondent velocity during this process

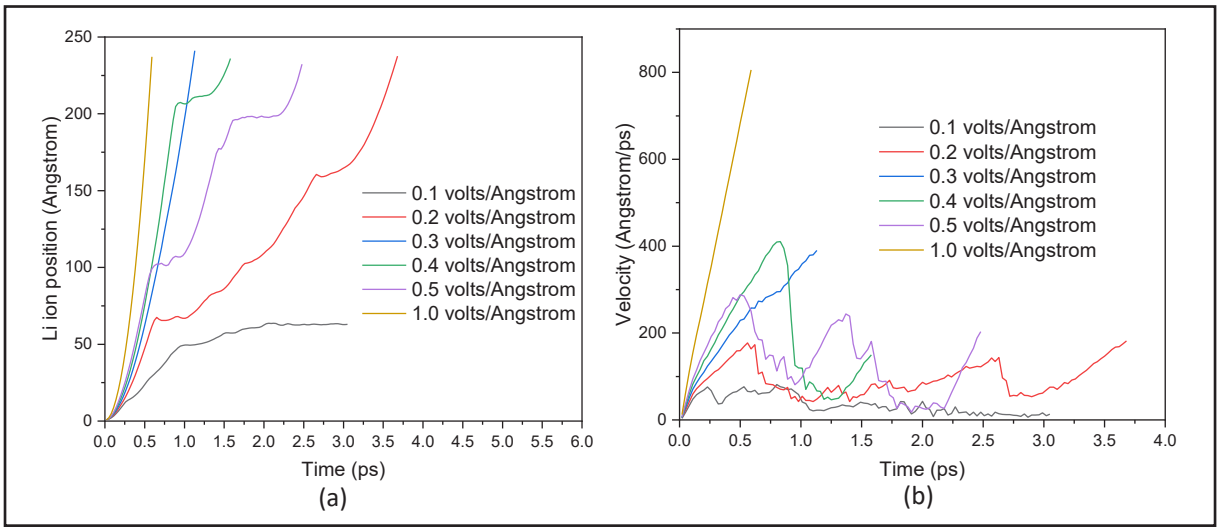

Source: Authors (2023)

The electric field with 0.1 volts/Å proved insufficient to overcome the Li diffusion energy barrier, resulting in them becoming stuck at approximately 50 Å. All other electric field strengths were found to be adequate for effectively moving the Li ions from the beginning of the channel to the end (approximately 230 Å). Interestingly, under the influence of electric fields of 1.0 and 0.3 volts/Å, the Li ions did not significantly interact with either the top or bottom layers, as observed in their position and velocity profiles (Fig. 7(a) and Fig. 7(b), respectively).

Although not shown, a similar procedure was conducted with Li positioned in the dirty lane. However, in this case, the ions collided with barriers, causing some Si atoms to be ejected with relatively high velocity in random directions. These ejected Si atoms eventually collided with other Si atoms belonging to the crystalline lattice, creating defects in these regions, which can negatively impact the use of silicene as an anode. Considering the results in Fig. 7, a strength of 0.2 volts/Å was chosen for the lithiation, i.e., the insertion of several Li ions into the silicene channel.

Figure 8 – Number of rings over time during lithiation

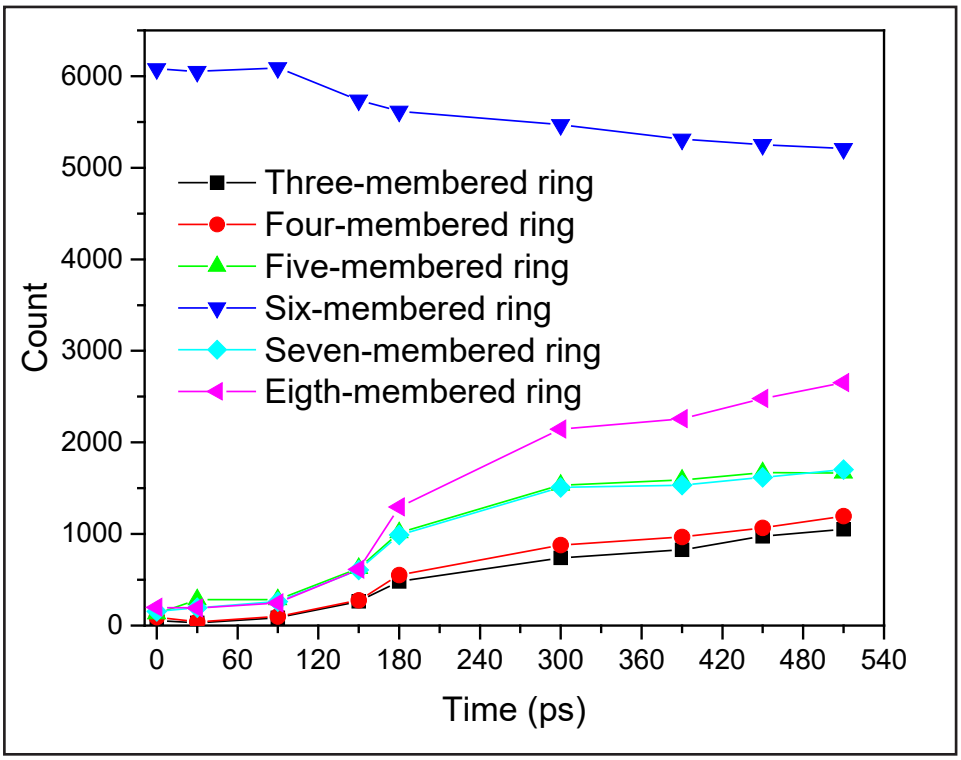

Source: Authors (2023)

While the Morse potential has been demonstrated not to significantly alter the crystalline structure of silicene with a single layer, dynamics change within the silicene channel due to adatom defects, as previously anticipated. During lithiation, ions are randomly introduced at the channel's outset, and over time, some encounter barriers caused by adatoms in the dirty path. With an increasing number of collisions, more defects emerge. Ultimately, the planar structure of silicene is compromised, revealing a disarray of Si and Li atoms. Figure 8 presents the profile of defect creation during lithiation, where is clearly observed the increase in defects, particularly in eight-membered ring types.

4 CONCLUSIONS

By using large-scale molecular dynamics simulations, this works investigated the Li ions behavior on a defective silicene grown on an Au substrate by VD technique, employing 2NN MEAN and Morse potential models. The crystallized silicene structure exhibited various defects, including large voids, adatoms, and rings with eight, seven, five, and four members.

In both potential models, it was observed that lithium ions preferentially positioned themselves at the center of rings with six or more elements, indicating a more stable state. However, rings with less than six elements led to ion instability due to the reduced available space, causing them to shift to the nearest ring with six or more elements. This process induces significant lattice deformation in silicene when using the 2NN MEAN potential, which is aggravated with the insertion of an electrical field into the system. This deformation is attributed to the potential's inability to accurately represent Si-Li pair interactions. In contrast, the Morse potential allowed ions to diffuse across the silicene surface without causing substantial deformation, rendering it more suitable for studying lithiation.

When introducing Li ions into a silicene channel with an electric field strength of 0.2 volts/Å — the minimum value needed to overcome the diffusion energy barrier

— damage to the silicene structure progressively occurred. Unlike the 2NN MEAN potential, this damage resulted from collisions between Li ions and Si adatoms. The affected adatoms are ejected at relatively high velocities in random directions before colliding with the silicene lattice.

The findings of this research suggest that employing silicene as a component in batteries may pose challenges when the silicene layer contains numerous defects, a common occurrence in experimental synthesis. Among these defects, adatoms are particularly detrimental, creating barriers during Li ion insertion. Therefore, experimental synthesis methods for silicene must minimize the occurrence of such defects to enhance its viability as anode in battery.

ACKNOWLEDGEMENTS

The authors thank the financial support from the Fundação de Amparo à Pesquisa do Estado do Rio de Janeiro (FAPERJ) – Processo SEI-260003/002235/2022 and SEI-260003/001582/2022 –, Conselho Nacional de Desenvolvimento Científico e Tecnológico (CNPq), and Coordenação de Aperfeiçoamento de Pessoal de Nível Superior – Brasil (CAPES) – Finance Code 001.

REFERENCES

Andrade, J. S., Bastos, I. N., Aliaga, L. C. R. (2021). Determinação das características estruturais e mecânicas da liga de alta entropia Hf-Nb-Ta-Zr. VETOR - Revista De Ciências Exatas E Engenharias, 30(2), 22–32. https://doi.org/10.14295/vetor.v30i2.13090.

Barboza, A. M., Aliaga, L. C. R., Faria, D., Bastos, I. N. (2022). Bilayer graphene kirigami. Carbon Trends, 9, 100227. https://doi.org/10.1016/j.cartre.2022.100227.

Barboza, A. M., Silva-Santos, J. A., Aliaga, L. C. R., Bastos, I. N., Faria, D. (2024). Silicene growth mechanisms on Au(111) and Au(110) substrates. Nanotechnology, 35, 165602. https://doi.org/10.1088/1361-6528/ad1aff.

Cherukara, M.J., Narayanan, B., Chan, H., and Sankaranarayanan, S. K. R. S. (2017). Silicene growth through island migration and coalescence. Nanoscale, 9, 10186–10192. https://doi.org/10.1039/C7NR03153J.

Cui, Z, Gao, F., and Qu, J. (2012). A second nearest-neighbor embedded atom method interatomic potential for Li–Si alloys. Journal of Power Sources, 207, 150–159. https://doi.org/10.1016/j.jpowsour.2012.01.145.

Feng, J.-W., Wang, H.-X., Zhao, J.-X., Cai, Q.-H., and Wang, X.-Z. (2014). Gas adsorption on silicene: A theoretical study. Computational Materials Science, 87, 218–226. https://doi.org/10.1016/j.commatsci.2014.02.025.

Galashev, A. Y., Ivanichkina, K., Katin, K., and Maslov, M. (2019). Computational Study of Lithium Intercalation in Silicene Channels on a Carbon Substrate after Nuclear Transmutation Doping. Computation, 7(4), 60–75. https://doi.org/10.3390/computation7040060.

Galashev, A. Y., Katin, K. P., and Maslov, M. M. (2019). Morse parameters for the interaction of metals with graphene and silicene. Physics Letters A, 383(2-3), 252–258. https://doi.org/10.1016/j.physleta.2018.10.025.

Galashev, A. Y., and Rakhmanova, O. R. (2019). Computer simulation of a forced drift of lithium ions through graphene membranes. High Temperature, 54, 11–19. https://doi.org/10.1134/S0018151X15050120.

Galashev, A. Y., Suzdaltsev, A. V., and Ivanichkina, K. A. (2020). Design of the high performance microbattery with silicene anode. Materials Science & Engineering B, 261, 114718. https://doi.org/10.1016/j.mseb.2020.114718.

Han, J., Li, H., and Yang, Q.-H. (2021). Compact energy storage enabled by graphenes: Challenges, strategies and progress. Materials today, 51, 552–565. https://doi.org/10.1016/j.mattod.2021.07.026.

Hirel, P. (2015). Atomsk: A tool for manipulating and converting atomic data files. Computer Physics Communications, 197, 212-219. https://doi.org/10.1016/j.cpc.2015.07.012.

Hüger, E., and Schmidt, H. (2018). Lithium permeability increase in nanosized amorphous silicon layers. Journal of Physical Chemistry C, 122(50), 28528–28536. https://doi.org/10.1021/acs.jpcc.8b09719.

Kim, Y.-M., Jung, I.-H., and Lee, B.-J. (2012). Atomistic modeling of pure Li and Mg–Li system. Modelling and Simulation in Materials Science and Engineering, 20, 035005. http://10.1088/0965-0393/20/3/035005.

Liu, J., Lyu, P., Nachtigall, P., and Xu, Y. (2018). Few-Layer Silicene Nanosheets with Superior Lithium- Storage Properties. Advanced Materials, 30, 1800838. https://doi.org/10.1002/adma.201800838.

Luo, X., Lang, J., Lv, S., and Li, Z. (2018). High performance sandwich structured Si thin film anodes with LiPON coating. Frontiers of Materials Science, 12, 147–155. https://doi.org/10.1007/s11706-018-0416-1.

Marom, R., Almaraj, S. F., Leifer, N., Jacob, D., and Aurbach, D. (2011). A review of advanced and practical lithium battery materials. Journal of Materials Chemistry, 21, 9938–9954. https://doi.org/10.1039/C0JM04225K.

Müser, M. H., Sukhomlinov, S. V., and Pastewka, L. (2022). Interatomic potentials: achievements and challenges. Advances in Physics: X, 8(1), 2093129. https://doi.org/10.1080/23746149.2022.2093129.

Salah, M., Murphy, P., Hall, C., Francis, C., Kerr, R., and Fabretto, M. (2019). Pure silicon thin-film anodes for lithium-ion batteries: A review. Journal of Power Sources, 414, 48–67. https://doi.org/10.1016/j.jpowsour.2018.12.068.

Sassa, Y., Johansson, F. O. L., Lindblad, A., Yazdi, M. G. et al. (2020). Kagome-like silicene: A novel exotic form of two-dimensional epitaxial silicon. Applied Surface Science, 530, 147195. https://doi.org/10.1016/j.apsusc.2020.147195.

Starikov, S., Lopanitsyna, N., Smirnova, D., and Makarov, S. (2018). Atomistic simulation of Si-Au melt crystallization with novel interatomic potential. Computational Materials Science, 142, 303–311. https://doi.org/10.1016/j.commatsci.2017.09.054.

Stukowski, A. (2010). Visualization and analysis of atomistic simulation data with OVITO the Open Visualization Tool. Modelling and Simulation in Materials Science and Engineering, 18, 015012. https://doi.org/10.1088/0965-0393/18/1/015012.

Tadmor, E. B., Elliott, R. S., Sethna, J. P., Miller, R. E., and C. A. Becker. (2011). The Potential of Atomistic Simulations and the Knowledgebase of Interatomic Models. JOM, 63, 17. https://doi.org/10.1007/s11837-011-0102-6.

Thompson, A.P., Aktulga, H.M., Berger, R. et al. (2022). LAMMPS - a flexible simulation tool for particle-based materials modeling at the atomic, meso, and continuum scales. Computer Physics Communications, 271, 10817. https://doi.org/10.1016/j.cpc.2021.108171.

You, Y., Yang, C., Zhang, X., Lin, H., and Shi, J. (2021). Emerging two-dimensional silicene nanosheets for biomedical applications. Materials Today Nano, 16, 100132. https://doi.org/10.1016/j.mtnano.2021.100132.

Zhao, J, Liu, H., Yu, Z., Quhe, R. et al. (2016). Rise of silicene: A competitive 2D material. Progress in Materials Science, 83, 24–151. https://doi.org/10.1016/j.pmatsci.2016.04.001.

Zhuang, J., Xu, X., Peleckis, G., Hao, W. et al. (2017). Silicene: A Promising Anode for Lithium-Ion Batteries. Advanced Materials, 29, 1606716. https://doi.org/10.1002/adma.201606716.

Authorship contributions

1 – Alexandre Melhorance Barboza

Universidade do Estado do Rio de Janeiro - PhD in computational modeling
https://orcid.org/0000-0001-6416-2138 - abarboza@iprj.uerj.br
Contribution: Conceptualization, Investigation, Methodology, Writing – original draft, Visualization, Project administration, Supervision

2 – Luis César Rodríguez Aliaga

Universidade do Estado do Rio de Janeiro - PhD Materials Science and Engineering
https://orcid.org/0000-0002-5397-674X - aliaga@iprj.uerj.br
Contribution: Methodology, Formal analysis, Writing – review & editing

3 – Daiara Fernandes de Faria

Universidade do Estado do Rio de Janeiro - PhD in Physics
https://orcid.org/0000-0001-5484-4506 - daiara@iprj.uerj.br
Contribution: Writing – review & editing, Validation

4 – Ivan Napoleão Bastos

Universidade do Estado do Rio de Janeiro - PhD in Metallurgical and Materials Engineering
https://orcid.org/0000-0001-7611-300X - inbastos@iprj.uerj.br
Contribution: Writing – review & editing, Resources, Funding acquisition

How to quote this article

Barboza, A. M., Aliaga, L. C. R., Faria, D. F. de, & Bastos, I. N. (2024). Dynamics of lithium ions on a silicene anode grown by vapor deposition using Morse and MEAM potentials. *Ciência e Natura,* 46, spe. 1, e86861. https://doi.org/10.5902/2179460X86861.